Letter

Spin Seebeck effect in nonmagnetic excitonic insulators

Joji Nasu [1] and Makoto Naka[2]
[1]*Department of Physics, Yokohama National University, Hodogaya, Yokohama 240-8501, Japan*
[2]*Waseda Institute for Advanced Study, Waseda University, Tokyo 169-8050, Japan*

(Received 29 November 2020; revised 10 February 2021; accepted 17 February 2021; published 5 March 2021)

We propose a mechanism of the spin Seebeck effect attributed to excitonic condensation in a nonmagnetic insulator. We analyze a half-filled two-orbital Hubbard model with a crystalline field splitting in the strong coupling limit. In this model, the competition between the crystalline field and electron correlations brings about an excitonic insulating state, where the two orbitals are spontaneously hybridized. Using the generalized spin-wave theory and Boltzmann transport equation, we find that a spin current generated by a thermal gradient is observed in the excitonic insulating state without magnetic fields. The spin Seebeck effect originates from spin-split collective excitation modes although the ground state does not exhibit any magnetic orderings. This peculiar phenomenon is inherent in the excitonic insulating state, whose order parameter is time-reversal odd and yields a spin splitting for the collective excitation modes. We also find that the spin current is strongly enhanced and its direction is inverted in the vicinity of the phase transition to another magnetically ordered phase. We suggest that the present phenomenon is possibly observed in perovskite cobaltites with the $GdFeO_3$-type lattice distortion.

DOI: 10.1103/PhysRevB.103.L121104

Spin current generation in insulating magnets has attracted considerable attention not only in modern condensed matter physics but also for applications to spintronic devices. While electric current cannot be produced in insulating magnets, spin current is successfully created by an applied thermal gradient, which is known as the spin Seebeck effect (SSE) [1–3]. The spin current is carried by spin-polarized collective excitations from a spin aligned ground state [4,5]. Therefore, materials showing the SSE have been explored in ferrimagnets and ferromagnets [6–9]. Recently, antiferromagnetic insulators and quantum spin liquid under magnetic fields are also considered as the candidates [10–13]. In contrast to these magnets, the SSE in nonmagnetic insulators remains elusive because spin-polarized excitations are not trivially present. Here, we focus on excitonic condensation instead of magnetic orderings to propose another type of the SSE.

The excitonic insulating (EI) state, where the conduction and valence bands are spontaneously hybridized by electron correlations, is a long-standing subject in condensed matter physics [14–22]. This state has been proposed to be realized in several multiorbital materials, e.g., transition metal oxides and chalcogenides [23–31]. Recently, it has been theoretically suggested that a carrier-doped excitonic magnet shows spin-split Fermi surfaces, which leads to spin current generation mediated by spin-polarized electrons [32–35]. This does not originate from the intrinsic spin-orbit coupling but is caused by the double-exchange mechanism [32]. On the other hand, this mechanism is absent in insulators. Meanwhile, the EI state is characterized by a certain order, which is not accompanied by magnetic orderings but is time-reversal broken [27–29,36–40]. Its order parameter gives rise to an effective internal field, which is expected to yield a spin splitting in the excitation spectra. However, spin transport properties in an undoped EI is not fully elucidated.

In this Letter, we investigate the spin excitations and transport properties of an EI state. We analyze an effective model derived from the two-orbital Hubbard model in the strong correlation limit, by using the generalized spin-wave theory (GSWT) and Boltzmann transport equation. We find that the collective spin excitations show a spin-dependent splitting in the nonmagnetic EI (NEI) state, which is a time-reversal broken state without magnetic dipole moments corresponding to a higher-order magnetic multipole order. As a result, a spin conductivity with respect to a thermal gradient becomes nonzero, i.e., the SSE appears, even without magnetic fields. This is attributed to the time-reversal symmetry breaking inherent in the NEI state. The spin conductivity substantially increases and its sign changes by temperature near the phase boundary to another EI state because of the softening of the spin-split mode. Finally, we propose how to verify our mechanism by presenting perovskite cobaltites with the $GdFeO_3$-type lattice distortion.

We start from the following two-orbital Hubbard model [41]: $\mathcal{H} = \mathcal{H}_U + \mathcal{H}_t$, where the Hamiltonians for local contributions and intersite electron hoppings are given by $\mathcal{H}_U = \Delta \sum_i n_{ia} + U \sum_{i\gamma} n_{i\gamma\uparrow} n_{i\gamma\downarrow} + U' \sum_i n_{ia} n_{ib} + J \sum_{i\sigma\sigma'} c^\dagger_{ia\sigma} c^\dagger_{ib\sigma'} c_{ia\sigma'} c_{ib\sigma} + I \sum_{i,\gamma\neq\gamma'} c^\dagger_{i\gamma\uparrow} c^\dagger_{i\gamma\downarrow} c_{i\gamma'\downarrow} c_{i\gamma'\uparrow}$ and $\mathcal{H}_t = \sum_{\langle ij\rangle\gamma\sigma} t_\gamma (c^\dagger_{i\gamma\sigma} c_{j\gamma\sigma} + \text{H.c.}) + V \sum_{\langle ij\rangle\sigma} (c^\dagger_{ia\sigma} c_{jb\sigma} + c^\dagger_{ib\sigma} c_{ja\sigma} + \text{H.c.})$, respectively. Here, $c^\dagger_{i\gamma\sigma}$ is the creation operator of the electron with spin $\sigma(=\uparrow,\downarrow)$ in orbital $\gamma(=a,b)$ at site i, and $n_{i\gamma} = \sum_\sigma c^\dagger_{i\gamma\sigma} c_{i\gamma\sigma}$ is the number operator. The crystalline field splitting, intraorbital and interorbital Coulomb interactions, Hund coupling, and pair

hopping interaction are represented by Δ, U, U', J, and I, respectively. In addition to the transfer integral t_γ between the γ orbitals in the nearest neighbor (NN) sites $\langle ij\rangle$ in $\mathcal{H}_t$, we consider the interorbital hopping V between the different orbitals in the NN sites.

In the present study, we focus on the electronic properties of the half-filling case in the strong correlation limit. The low-energy local eigenstates for $\mathcal{H}_U$ are the low-spin (LS) state $|L\rangle = (f c^\dagger_{b\uparrow} c^\dagger_{b\downarrow} - g c^\dagger_{a\uparrow} c^\dagger_{a\downarrow})|\emptyset\rangle$, where $f = \sqrt{(1+\Delta/\Delta')/2}$ and $g = \sqrt{(1-\Delta/\Delta')/2}$ with $\Delta' = \sqrt{\Delta^2 + I^2}$, and three high-spin (HS) states $\{|X\rangle, |Y\rangle, |Z\rangle\}$, which are given by $|X\rangle = \frac{1}{\sqrt{2}}(-c^\dagger_{a\uparrow} c^\dagger_{b\uparrow} + c^\dagger_{a\downarrow} c^\dagger_{b\downarrow})|\emptyset\rangle$, $|Y\rangle = \frac{i}{\sqrt{2}}(c^\dagger_{a\uparrow} c^\dagger_{b\uparrow} + c^\dagger_{a\downarrow} c^\dagger_{b\downarrow})|\emptyset\rangle$, and $|Z\rangle = \frac{1}{\sqrt{2}}(c^\dagger_{a\uparrow} c^\dagger_{b\downarrow} + c^\dagger_{a\downarrow} c^\dagger_{b\uparrow})|\emptyset\rangle$. Here, $|\emptyset\rangle$ stands for the vacuum. The effective model is defined for the subspace composed of the direct product of these four local states. Using the second-order perturbation expansion with respect to $\mathcal{H}_t$, the low-energy Hamiltonian is obtained as

$$\begin{aligned}\mathcal{H}_{\rm eff} = &-\Delta_z \sum_i \tau^z_i + J_z \sum_{\langle ij\rangle} \tau^z_i \tau^z_j + J_s \sum_{\langle ij\rangle} \boldsymbol{S}_i \cdot \boldsymbol{S}_j \\ &- J_x \sum_{\langle ij\rangle\Gamma} \tau^x_{\Gamma i} \tau^x_{\Gamma j} - J_y \sum_{\langle ij\rangle\Gamma} \tau^y_{\Gamma i} \tau^y_{\Gamma j} \\ &- K \sum_{\langle ij\rangle\Gamma} \left(S^\Gamma_i \tau^x_{\Gamma j} + \tau^x_{\Gamma i} S^\Gamma_j \right), \end{aligned} \tag{1}$$

where the exchange constants, Δ_z, J_s, J_x, J_y, and K are determined by the parameters in $\mathcal{H}$ [42]. In the effective model, S^X_i, S^Y_i, and S^Z_i represent the spin-1 operators at site i for the HS states, and the pseudospins τ^x_Γ, τ^y_Γ ($\Gamma = X, Y, Z$), and τ^z describe the matrix elements between LS and HS states, where $\tau^x_\Gamma = |L\rangle\langle\Gamma| + |\Gamma\rangle\langle L|$, $\tau^y_\Gamma = i(|L\rangle\langle\Gamma| - |\Gamma\rangle\langle L|)$, and $\tau^z = \sum_\Gamma (|\Gamma\rangle\langle\Gamma| - |L\rangle\langle L|)$, respectively. Note that τ^z represents the energy difference between LS and HS states, and τ^x_Γ and τ^y_Γ yield the hybridization between these states. Therefore, nonzero expectation values of τ^x_Γ and τ^y_Γ indicate the emergence of the EI state. In particular, the former (latter) is the time-reversal odd (even) operator, and therefore, τ^x_Γ can couple with the spin operators as shown in Eq. (1), where the coupling constant K is proportional to $(t_a + t_b)V$; K is nonzero in the presence of the interorbital hopping [42]. In the following calculations, we study the system with the direct gap, $t_a t_b < 0$. In this case, the exchange constants J_x and J_y satisfy the relation $J_x \gtrsim J_y$ and J_x is positive. This leads to the ferrotype pseudospin correlation while the spin exchange constant J_s is always antiferromagnetic.

To analyze the spin excitations and transport properties in the Hamiltonian Eq. (1), we apply the GSWT [42–49]. In this method, the mean-field (MF) approximation is applied, and the Hamiltonian is divided into $\mathcal{H}_{\rm eff} = \sum_i \mathcal{H}^{\rm MF}_i + \mathcal{H}'$; $\mathcal{H}^{\rm MF}_i$ is the local MF Hamiltonian obtained by the decoupling of the exchange interactions and $\mathcal{H}'$ is the contribution beyond the MF Hamiltonian. $\mathcal{H}'$ is given by the interactions between the fluctuation around the MFs, $\delta O_i = O_i - \langle 0; C_i|O|0; C_i\rangle$, where $|0; C_i\rangle$ is the local MF ground state of $\mathcal{H}^{\rm MF}_i$ on sublattice C_i to which site i belongs. In the GSWT, this is approximated as $\delta O_i \simeq \sum_n \langle n; C_i|O|0; C_i\rangle a^\dagger_{in} + {\rm H.c.}$, where $a^\dagger_{in}$ is a creation operator of a boson, where the summation for n is taken for the local excited states of $\mathcal{H}^{\rm MF}_i$. By the above procedure, $\mathcal{H}_{\rm eff}$ is approximated as $\mathcal{H}_{\rm SW}$, which is written as a bilinear form of the bosons $a^\dagger_{in}$ [42]. This is diagonalized by the Bogoliubov transformation [50]. We introduce a new bosonic operator $\alpha^\dagger_{\boldsymbol{q}\eta}$ with the excitation energy $\omega_{\boldsymbol{q}\eta}$ for the wave vector $\boldsymbol{q}$ and branch η. Using the GSWT, we calculate the dynamical spin correlator [36,42]

$$\mathcal{S}^{\Gamma\Gamma'}(\boldsymbol{q}, \omega) = \frac{1}{2\pi} \int_{-\infty}^{\infty} dt \, \langle\langle 0|\delta S^\Gamma_{\boldsymbol{q}}(t) \delta S^{\Gamma'}_{-\boldsymbol{q}}|0\rangle\rangle e^{i\omega t - \delta|t|}, \tag{2}$$

where $\delta S^\Gamma_{\boldsymbol{q}} = N^{-1/2} \sum_i \delta S^\Gamma_i e^{-i\boldsymbol{q}\cdot\boldsymbol{r}_i}$, $O(t) = e^{i\mathcal{H}_{\rm SW} t} O e^{-i\mathcal{H}_{\rm SW} t}$, δ is a broadening factor, and $|0\rangle\rangle$ is the vacuum for the Bogoliubov bosons.

The thermal conductivity $\kappa \equiv \kappa^{xx}_E$ and spin conductivity with respect to a thermal gradient, $\kappa_s \equiv \kappa^{xx}_{S^z}$, are defined by $\langle J^\mu_{\mathcal{O}}\rangle_{\nabla T}/V = \kappa^{\mu\nu}_{\mathcal{O}}(-\nabla_\nu T)$, where V is the volume, $\langle\cdots\rangle_{\nabla T}$ represents the expectation value in the presence of the thermal gradient, and $\mu, \nu = x, y, z$ stand for the coordinate axes. The energy current $\boldsymbol{J}_E$ is defined from the energy polarization $\boldsymbol{P}_E = \sum_i \boldsymbol{r}_i h_i$ as $\boldsymbol{J}_E = i[\mathcal{H}_{\rm SW}, \boldsymbol{P}_E]$, where h_i is composed of the terms involving site i in $\mathcal{H}_{\rm SW}$ [51–53]. The spin current $J^\mu_{S^Z}$ is also defined in a similar manner. The spin polarization is introduced as $\boldsymbol{P}_{S^Z} = \sum_i \boldsymbol{r}_i S^Z_i \simeq \sum_{in} \boldsymbol{r}_i \langle n; C_i|\delta S^Z_i|n; C_i\rangle a^\dagger_{in} a_{in} +$ const. when S^z_i commutes with $\mathcal{H}^{\rm MF}_i$ because the spin-orbit coupling is not taken into account in Eq. (1). The conductivities are calculated using the Boltzmann equation with the relaxation time approximation [3,42,54,55]. We have numerically confirmed that the results are consistent with those obtained by the Kubo formula [11,56].

First, we show the results of the two-sublattice MF approximation for Eq. (1) on a square lattice, where the length of the primitive translation vectors is set to be unity. The ground-state MF phase diagrams without the interorbital hopping, i.e., at $K = 0$, have been already examined in Ref. [36]. In the present calculations, we choose the exchange parameters as $(J_s, J_x, J_y, J_z)/J_s = (1, 0.5, 0, 0.1)$. Figure 1 shows the Δ_z dependences of the HS density $\bar{n}_H$ and the spin and pseudospin moments at $K/J_s = 0.1$. We find the four phases, the uniform LS, HS with the AFM order, and two-types of EI phases: the NEI and magnetic EI (MEI) [57]. Here, the uniform and staggard spin moments are introduced as $S^\Gamma_\pm = \frac{1}{2}(\langle S^\Gamma\rangle_A \pm \langle S^\Gamma\rangle_B)$ with $\langle S^\Gamma\rangle_A$ and $\langle S^\Gamma\rangle_B$ being the moments on the sublattices A and B, respectively. The pseudospin moments, $\tau^x_{\Gamma\pm}$ and $\tau^y_{\Gamma\pm}$, are defined in the same manner. The LS (HS) phase is characterized by $\bar{n}_H = 0$ ($\bar{n}_H = 1$) as shown in Fig. 1(a) and $\bar{n}_H$ continuously changes in the NEI and MEI phases. In the HS phase, $S^X_- = 1$, indicating the AFM order for S^X [Fig. 1(b)]. The MEI phase also possesses nonzero S^X_- and small FM S^Z components. Accompanied by the spin canting, $\tau^x_{X\pm}$ takes a small value [Fig. 1(c)] in the MEI state while it is zero at $K = 0$. On the other hand, in the NEI phase, only $\tau^x_{Z\pm}$ is finite, similar to the case with $K = 0$. We find the phase boundaries are almost unchanged by the introduction of K.

While the MF ground state in the NEI is not changed qualitatively by K, we find the substantial change of the spin excitation spectrum. As shown in Fig. 2(a), there are four excitation modes in the NEI phase at $K = 0$. The low-energy two gapless modes and high-energy two gapped modes correspond

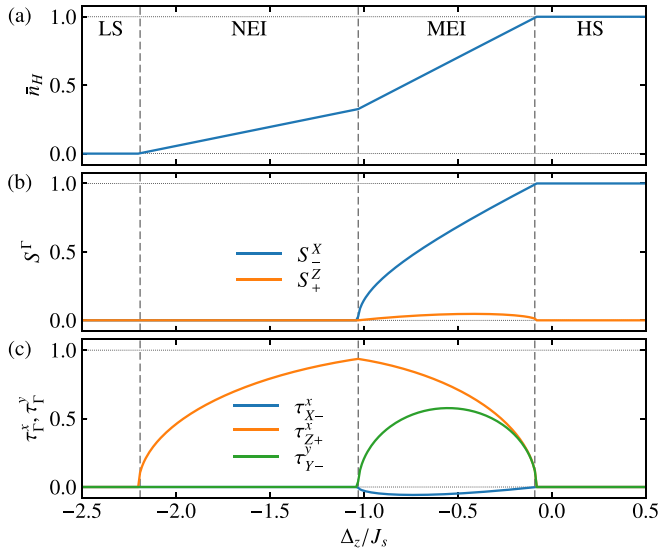

FIG. 1. (a) High-spin density $\bar{n}_H$, (b) spin moments $S^\Gamma_\pm$, and (c) pseudospin moments, $\tau^x_{\Gamma\pm}$ and $\tau^y_{\Gamma\pm}$, as functions of Δ_z with the exchange parameters $(J_x, J_y, J_z, K)/J_s = (0.5, 0, 0.1, 0.1)$. The dashed lines indicate the phase boundaries.

to the spin and orbital excitations, respectively [36]. To examine the spin dependence of the collective modes, we calculate the imaginary part of the dynamical spin correlator $\mathcal{S}^{YX}(\boldsymbol{q}, \omega)$ [58]. Note that $\mathrm{Im}\mathcal{S}^{YX}(\boldsymbol{q}, \omega) = [\mathcal{S}^{-+}(\boldsymbol{q}, \omega) - \mathcal{S}^{+-}(\boldsymbol{q}, \omega)]/4$, where $S^\pm = S^X \pm iS^Y$. This expression clearly indicates that the positive (negative) spectral weight corresponds to the spin excitation associated with a positive (negative) change of S^Z. Figure 2 shows the contour map of $\mathrm{Im}\mathcal{S}^{YX}(\omega)$ and dispersion relations of the collective excitations for several values of K and Δ_z. As shown in Figs. 2(a)–2(c), in the NEI phase with $\Delta_z/J_s = -1.2$, one of the spin excitation modes splits into two by the introduction of K. These two modes are associated with the positive and negative weights of $\mathrm{Im}\mathcal{S}^{YX}(\boldsymbol{q}, \omega)$. This indicates that the spin splitting of the collective modes is caused by the interorbital hopping, i.e., K, although the EI state remains nonmagnetic [see Fig. 1(b)]. In the NEI state, the uniform pseudospin moment for $\langle\tau^x_Z\rangle$ is nonzero, resulting in the effective magnetic field for S^Z by the last term of Eq. (1). This effective field does not induce any local spin moments in the ground state but gives rise to the spin splitting in the excited states [59].

We also find that the spin-split collective modes are softened while Δ_z approaching the critical point between the NEI and MEI phases, $\Delta_z^{\mathrm{critical}} \simeq \Delta_z = 1.0312J_s$ [Figs. 2(c) and 2(d)]. At this point, one of these modes is gapless at the M point in the Brillouin zone with a quadratic dispersion. In the MEI phase above $\Delta_z^{\mathrm{critical}}$, and two gapless linear dispersions with different velocities appear [36]. In the MEI phase, while increasing Δ_z, the low-energy weight of $\mathrm{Im}\mathcal{S}^{YX}(\omega)$ turns from positive to negative [Figs. 2(e) and 2(f)].

Keeping this in mind, let us examine spin transport properties in the EI phases when a thermal gradient is applied to the system. Figure 3(a) shows the temperature dependence of the spin conductivity κ_s in the NEI phase [60]. In the NEI phase at $\Delta_z/J_s = -1.25$ far from $\Delta_z^{\mathrm{critical}}$, κ_s/τ is negative and decreases with increasing temperature. This is understood as follows. As shown in Figs. 2(b) and 2(c), the group velocity of the collective mode with the negative weight of $\mathrm{Im}\mathcal{S}^{YX}(\omega)$ is larger than that with the positive weight around the Γ point. This implies that the large group velocity of the spin excitation decreasing S^Z contributes dominantly to the spin transport rather than a higher occupation of the lower branch, and hence, κ_s is negative.

At $\Delta_z/J_s = -1.2$, κ_s/τ turns to increase with increasing temperature and its sign changes by the temperature evolution. Further increase of Δ_z enhances the spin conductivity strongly in the high temperature region. At the critical point $\Delta_z^{\mathrm{critical}}$, κ_s/τ largely increases proportional to temperature as shown in the inset of Fig. 3(a). The peculiar temperature dependence is attributed to the softening of the spin-split collective mode at the M point as shown in Fig. 2(d). This mode is associated with the positive $\mathrm{Im}\mathcal{S}^{YX}(\omega)$, indicating the excitation with raising S^Z, and therefore, κ_s becomes positive near $\Delta_z^{\mathrm{critical}}$. In the MEI phase, our formalism is not applicable for calculating κ_s [60] but we expect that κ_s changes to positive to negative while increasing Δ_z from $\Delta_z^{\mathrm{critical}}$ on the basis of the low energy behavior of $\mathrm{Im}\mathcal{S}^{YX}(\omega)$ shown in Figs. 2(d)–2(f).

To examine the conversion ratio from the thermal to spin current, we calculate κ_s/κ, which does not depend on τ in the present approximation. The results are shown in Fig. 3(b). At $\Delta_z/J_s = -1.25$, this quantity is negative but the sign change is seen in the case close to $\Delta_z^{\mathrm{critical}}$. While κ_s/κ approaches a negative common value in the low temperature limit in the

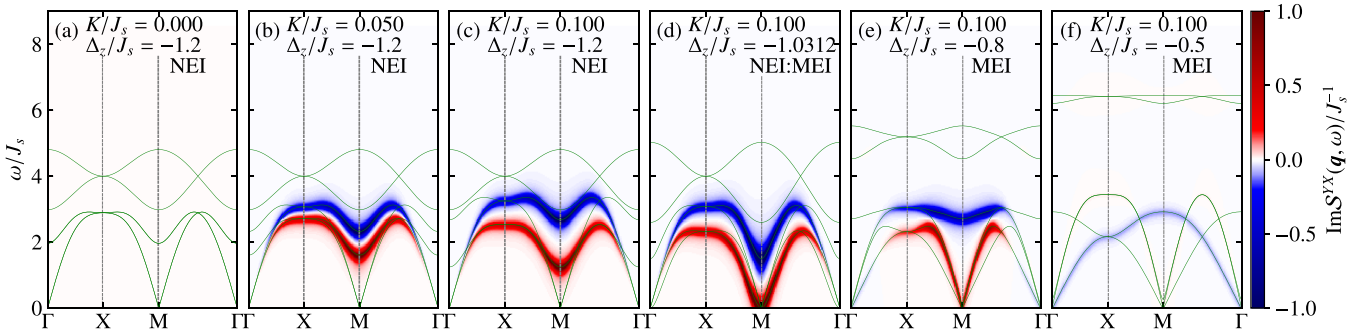

FIG. 2. Contour plots of the imaginary parts of the dynamical spin correlator, $\mathrm{Im}\mathcal{S}^{YX}(\omega)$, with $\delta = 0.1J$ at several parameters. Green lines represent the excitation energies.

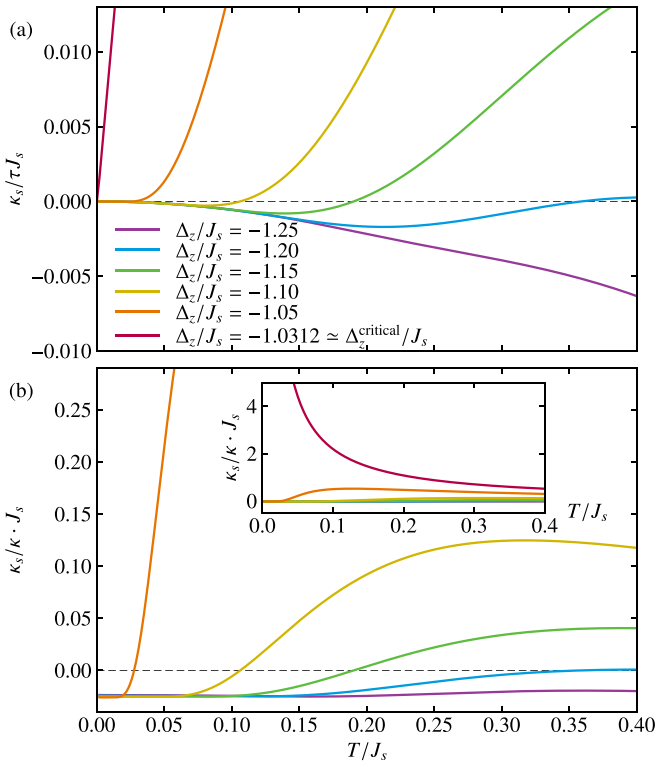

FIG. 3. Temperature dependences of (a) the spin conductivity κ_s and (b) the ratio κ_s/κ at several Δ_z in the NEI phase with the exchange parameters $(J_x, J_y, J_z, K)/J_s = (0.5, 0, 0.1, 0.1)$, where τ is the relaxation time. The inset of (b) is its extended plot.

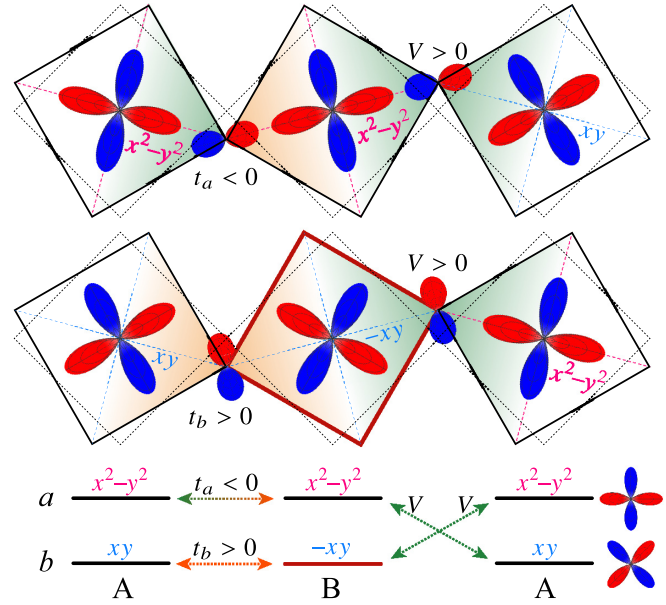

FIG. 4. Schematic pictures of orbital configurations in the $GdFeO_3$-type distortion to understand the correspondence to the present model. The p orbitals are also depicted on the coordinate of the middle octahedra. The gauge transformation for the d_{xy} orbital to $-d_{xy}$ are applied to the octahedron surrounded by the red line. The orange and green colors in the octahedra represent the positive and negative d-p hybridizations, respectively. Transfer integrals between the same and different orbitals are shown in the bottom.

NEI phase, the different behavior is observed at $\Delta_z^{\rm critical}$; κ_s/κ appears to diverge with decreasing temperature as shown in the inset of Fig. 3(b).

Here, we discuss how to verify our theoretical proposal in real materials. One of the candidates of EIs is the perovskite cobaltite $Pr_{0.5}Ca_{0.5}CoO_3$. This material exhibits a metal-insulator transition at about 90 K and magnetic orderings have not been observed experimentally [61–63]. The Co ions are expected to be trivalent and multiple spin states such as LS (t_{2g}^6) and HS ($t_{2g}^4 e_g^2$) are energetically competing. It was suggested that the NEI state with the spontaneous hybridization occurs between $d_{x^2-y^2}$ and d_{xy} orbitals by first principles calculations [27–29]. Therefore, the present two-orbital Hubbard model is a minimal model to capture the nature of the EI state in the material. The space group of $Pr_{0.5}Ca_{0.5}CoO_3$ is orthorhombic (*Pnma*) with the $GdFeO_3$-type distortion in both higher and lower temperatures [63–65]. The detailed structure analysis suggested that the rotation of CoO_6 octahedra corresponding to the $GdFeO_3$-type distortion is enhanced with decreasing temperature. This distortion gives rise to the intersite interorbital hopping between the $d_{x^2-y^2}$ in the e_g orbitals and d_{xy} in the t_{2g} orbitals as shown in Fig. 4. This effect is incorporated as V in the two-orbital Hubbard model, which is different from the previous studies [32–35]. By applying the gauge transformation for the b orbital in the B sublattice, the Hamiltonian is mapped onto the case with the uniform interorbital hopping and $t_a t_b < 0$, which is nothing but the system addressed by the present study. This transformation does not affect the spin operators and eigenenergies, and therefore, the results for the spin-split excitations and SSE are expected to be observed in the real material $Pr_{0.5}Ca_{0.5}CoO_3$ if the excitonic order is realized.

As shown in Fig. 3(b), despite the absence of magnetic orders and magnetic fields, the order of κ_s is close to that of κ in natural units, which is similar to the case of ferromagnetic Heisenberg models. Since the SSE mediated by the collective excitations has been measured in ferromagnetic/ferrimagnetic insulators such as iron-based garnets [6,7], we expect that the spin current is observed when the EI state is realized in the candidate material. Furthermore, in the iron-based garnets, spin-dependent magnons were observed by inelastic neutron scattering measurements [66]. Therefore, we believe that the SSE and spin splitting in collective excitations can be measured experimentally in candidate materials of the EI state although its order parameter is a higher-order multipole [27,36,37], which is difficult to be observed by conventional probes.

In summary, we have proposed a mechanism of the spin Seebeck effect in a nonmagnetic excitonic insulating state by analyzing the effective model derived from the two-orbital Hubbard model in the strong correlation limit. We have revealed that the spin Seebeck effect originates from the spin-split collective excitations, which is caused by an internal effective field emerging from the excitonic order parameter. We have also suggested that these phenomena will be experimentally observed in perovskite cobaltites with the $GdFeO_3$-type distortion.

The authors thank S. Ishihara, Y. Ohta, K. Sugimoto, and S. Yamamoto for fruitful discussions. Parts of the numerical calculations were performed in the supercomputing systems in ISSP, the University of Tokyo. This work was supported by a Grant-in-Aid for Scientific Research from JSPS, KAKENHI Grant No. JP19K03723.

[1] J. Xiao, G. E. W. Bauer, K. Uchida, E. Saitoh, and S. Maekawa, Phys. Rev. B **81**, 214418 (2010).
[2] H. Adachi, J. Ohe, S. Takahashi, and S. Maekawa, Phys. Rev. B **83**, 094410 (2011).
[3] S. M. Rezende, R. L. Rodríguez-Suárez, R. O. Cunha, A. R. Rodrigues, F. L. A. Machado, G. A. Fonseca Guerra, J. C. Lopez Ortiz, and A. Azevedo, Phys. Rev. B **89**, 014416 (2014).
[4] S. Maekawa, H. Adachi, K. Uchida, J. Ieda, and E. Saitoh, J. Phys. Soc. Jpn. **82**, 102002 (2013).
[5] H. Adachi, K. Uchida, E. Saitoh, and S. Maekawa, Rep. Prog. Phys. **76**, 036501 (2013).
[6] K. Uchida, J. Xiao, H. Adachi, J. Ohe, S. Takahashi, J. Ieda, T. Ota, Y. Kajiwara, H. Umezawa, H. Kawai *et al.*, Nat. Mater. **9**, 894 (2010).
[7] K. Uchida, H. Adachi, T. Ota, H. Nakayama, S. Maekawa, and E. Saitoh, Appl. Phys. Lett. **97**, 172505 (2010).
[8] S. S.-L. Zhang and S. Zhang, Phys. Rev. Lett. **109**, 096603 (2012).
[9] S. S.-L. Zhang and S. Zhang, Phys. Rev. B **86**, 214424 (2012).
[10] Z. Qiu, D. Hou, J. Barker, K. Yamamoto, O. Gomonay, and E. Saitoh, Nat. Mater. **17**, 577 (2018).
[11] M. Naka, S. Hayami, H. Kusunose, Y. Yanagi, Y. Motome, and H. Seo, Nat. Commun. **10**, 4305 (2019).
[12] D. Hirobe, M. Sato, T. Kawamata, Y. Shiomi, K.-i. Uchida, R. Iguchi, Y. Koike, S. Maekawa, and E. Saitoh, Nat. Phys. **13**, 30 (2017).
[13] T. Minakawa, Y. Murakami, A. Koga, and J. Nasu, Phys. Rev. Lett. **125**, 047204 (2020).
[14] N. F. Mott, Philos. Mag. **6**, 287 (1961).
[15] D. Jérome, T. M. Rice, and W. Kohn, Phys. Rev. **158**, 462 (1967).
[16] B. I. Halperin and T. M. Rice, Rev. Mod. Phys. **40**, 755 (1968).
[17] L. Balents, Phys. Rev. B **62**, 2346 (2000).
[18] C. D. Batista, Phys. Rev. Lett. **89**, 166403 (2002).
[19] J. Kuneš, J. Phys.: Condens. Matter **27**, 333201 (2015).
[20] S. Mase and T. Sakai, J. Phys. Soc. Jpn. **31**, 730 (1971).
[21] H. Fukuyama and T. Nagai, J. Phys. Soc. Jpn. **31**, 812 (1971).
[22] Y. Kuramoto and M. Morimoto, J. Phys. Soc. Jpn. **44**, 1759 (1978).
[23] Y. Wakisaka, T. Sudayama, K. Takubo, T. Mizokawa, M. Arita, H. Namatame, M. Taniguchi, N. Katayama, M. Nohara, and H. Takagi, Phys. Rev. Lett. **103**, 026402 (2009).
[24] Y. Wakisaka, T. Sudayama, K. Takubo, T. Mizokawa, N. L. Saini, M. Arita, H. Namatame, M. Taniguchi, N. Katayama, M. Nohara, and H. Takagi, J. Supercond. Nov. Magn. **25**, 1231 (2012).
[25] T. Kaneko, T. Toriyama, T. Konishi, and Y. Ohta, Phys. Rev. B **87**, 035121 (2013).
[26] T. Kaneko and Y. Ohta, Phys. Rev. B **90**, 245144 (2014).
[27] J. Kuneš and P. Augustinský, Phys. Rev. B **90**, 235112 (2014).
[28] J. Kuneš and P. Augustinský, Phys. Rev. B **89**, 115134 (2014).
[29] A. Sotnikov and J. Kuneš, Phys. Rev. B **96**, 245102 (2017).
[30] A. Ikeda, T. Nomura, Y. H. Matsuda, A. Matsuo, K. Kindo, and K. Sato, Phys. Rev. B **93**, 220401(R) (2016).
[31] A. Ikeda, Y. H. Matsuda, and K. Sato, Phys. Rev. Lett. **125**, 177202 (2020).
[32] J. Kuneš and D. Geffroy, Phys. Rev. Lett. **116**, 256403 (2016).
[33] D. Geffroy, A. Hariki, and J. Kuneš, Phys. Rev. B **97**, 155114 (2018).
[34] H. Nishida, S. Miyakoshi, T. Kaneko, K. Sugimoto, and Y. Ohta, Phys. Rev. B **99**, 035119 (2019).
[35] S. Yamamoto, K. Sugimoto, and Y. Ohta, Phys. Rev. B **101**, 174428 (2020).
[36] J. Nasu, T. Watanabe, M. Naka, and S. Ishihara, Phys. Rev. B **93**, 205136 (2016).
[37] T. Kaneko and Y. Ohta, Phys. Rev. B **94**, 125127 (2016).
[38] M. M. Altarawneh, G.-W. Chern, N. Harrison, C. D. Batista, A. Uchida, M. Jaime, D. G. Rickel, S. A. Crooker, C. H. Mielke, J. B. Betts, J. F. Mitchell, and M. J. R. Hoch, Phys. Rev. Lett. **109**, 037201 (2012).
[39] T. Tatsuno, E. Mizoguchi, J. Nasu, M. Naka, and S. Ishihara, J. Phys. Soc. Jpn. **85**, 083706 (2016).
[40] A. Sotnikov and J. Kuneš, Sci. Rep. **6**, 30510 (2016).
[41] P. Werner and A. J. Millis, Phys. Rev. Lett. **99**, 126405 (2007).
[42] See Supplemental Material at http://link.aps.org/supplemental/10.1103/PhysRevB.103.L121104 for the derivation of the effective Hamiltonian, details of the generalized spin wave theory, and derivation of the transport coefficients using the generalized spin wave theory.
[43] F. P. Onufrieva, Zh. Eksp. Teor. Fiz **89**, 2270 (1985) [Sov. Phys. JETP **62**, 1311 (1985)].
[44] N. Papanicolaou, Nucl. Phys. B **305**, 367 (1988).
[45] H. Kusunose and Y. Kuramoto, J. Phys. Soc. Jpn. **70**, 3076 (2001).
[46] R. Shiina, H. Shiba, P. Thalmeier, A. Takahashi, and O. Sakai, J. Phys. Soc. Jpn. **72**, 1216 (2003).
[47] A. Joshi, M. Ma, F. Mila, D. N. Shi, and F. C. Zhang, Phys. Rev. B **60**, 6584 (1999).
[48] Y. Murakami, T. Oka, and H. Aoki, Phys. Rev. B **88**, 224404 (2013).
[49] J. Nasu and S. Ishihara, Phys. Rev. B **88**, 205110 (2013).
[50] J. H. P. Colpa, Physica A **93**, 327 (1978).
[51] H. Katsura, N. Nagaosa, and P. A. Lee, Phys. Rev. Lett. **104**, 066403 (2010).
[52] R. Matsumoto and S. Murakami, Phys. Rev. Lett. **106**, 197202 (2011).
[53] R. Matsumoto, R. Shindou, and S. Murakami, Phys. Rev. B **89**, 054420 (2014).
[54] S. M. Rezende, R. L. Rodríguez-Suárez, and A. Azevedo, Phys. Rev. B **93**, 014425 (2016).
[55] R. Takashima, Y. Shiomi, and Y. Motome, Phys. Rev. B **98**, 020401(R) (2018).
[56] M. Ogata and H. Fukuyama, J. Phys. Soc. Jpn. **86**, 094703 (2017).

[57] The NEI and MEI were introduced in Ref. [36] as EIQ and EIM, respectively.

[58] J. Barker and G. E. W. Bauer, Phys. Rev. Lett. **117**, 217201 (2016).

[59] When one changes the sign of K or the EI order parameter $\langle \tau_Z^x \rangle$, the sign of $\mathrm{Im}\mathcal{S}^{YX}(\boldsymbol{q}, \omega)$ is inverted.

[60] Note that κ_s is valid only for the case with the conservation of the total S^Z in $\mathcal{H}_{\mathrm{SW}}$ [42]. We calculate this in the NEI phase but do not in the MEI phase, because the spin current does not have a conserved current in the MEI phase due to the small spin canting.

[61] T. Fujita, T. Miyashita, Y. Yasui, Y. Kobayashi, M. Sato, E. Nishibori, M. Sakata, Y. Shimojo, N. Igawa, Y. Ishii, K. Kakurai, T. Adachi, Y. Ohishi, and M. Takata, J. Phys. Soc. Jpn. **73**, 1987 (2004).

[62] J. Hejtmánek, Z. Jirák, O. Kaman, K. Knížek, E. Šantavá, K. Nitta, T. Naito, and H. Fujishiro, Eur. Phys. J. B **86**, 305 (2013).

[63] S. Tsubouchi, T. Kyômen, M. Itoh, P. Ganguly, M. Oguni, Y. Shimojo, Y. Morii, and Y. Ishii, Phys. Rev. B **66**, 052418 (2002).

[64] S. Tsubouchi, T. Kyômen, M. Itoh, and M. Oguni, Phys. Rev. B **69**, 144406 (2004).

[65] J. Hejtmánek, E. Šantavá, K. Knížek, M. Maryško, Z. Jirák, T. Naito, H. Sasaki, and H. Fujishiro, Phys. Rev. B **82**, 165107 (2010).

[66] Y. Nambu, J. Barker, Y. Okino, T. Kikkawa, Y. Shiomi, M. Enderle, T. Weber, B. Winn, M. Graves-Brook, J. M. Tranquada, T. Ziman, M. Fujita, G. E. W. Bauer, E. Saitoh, and K. Kakurai, Phys. Rev. Lett. **125**, 027201 (2020).